

## Oxygen-Initiated Free-Radical Polymerization of Alkyl Acrylates at High Temperatures

Shi Liu,<sup>#</sup> Lauren Chua,<sup>#</sup> Ahmad Arabi Shamsabadi, Patrick Corcoran, Abhirup Patra, Michael C. Grady, Masoud Soroush,<sup>\*</sup> and Andrew M. Rappe<sup>\*</sup>

**Cite This:** *Macromolecules* 2021, 54, 7925–7930

**Read Online**

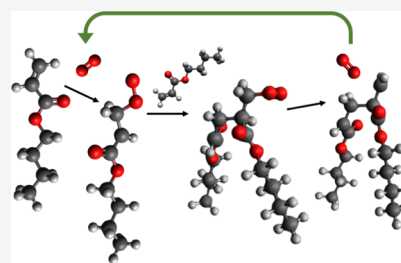
ACCESS |

Metrics & More

Article Recommendations

Supporting Information

**ABSTRACT:** Molecular oxygen has been reported to be a strong inhibitor at low temperatures. Here, it is shown that the introduction of oxygen gas into the free-radical polymerization of *n*-butyl acrylate (*n*BA) results in high conversion of the monomer in a very short time at temperatures above 140 °C without the use of any conventional initiators. By conducting first-principles calculations based on density functional theory, this work for the first time identifies and kinetically studies the most-likely reactions via which molecular oxygen contributes to polymer chain initiation. It provides theoretical and experimental evidence that molecular oxygen acts as a catalyst in alkyl acrylate free-radical polymerization at high temperatures. A triplet diradical intermediate is generated from solvated oxygen reacting with an alkyl acrylate monomer. The intermediate then reacts with another monomer and thermally dissociates from molecular oxygen to proceed toward polymerization. This theoretical finding is supported by laboratory experiments showing that in the presence of a very small amount of molecular oxygen and in the absence of any thermal initiators, free-radical polymerization of *n*BA occurs sustainably and proceeds to a very high monomer conversion. This work opens a new path for a more economic and sustainable production of higher-quality acrylic polymers using molecular oxygen as an initiator catalyst.



### INTRODUCTION

Acrylic polymers are used in many products such as paints, coatings, adhesives, fibers, plastics, and cosmetic products. Severe restrictions placed on volatile organic compounds prevent the use of high solvent concentrations, which improve performance during application, in paints and coatings.<sup>1</sup> Therefore, high-temperature (120–220 °C) polymerization processes are employed to synthesize lower average molecular-weight polymers that require less solvent while maintaining brushability. At high temperatures, the rates of secondary reactions such as monomer self-initiation, depropagation, and  $\beta$ -scission are appreciable and produce resins with low average molecular weights.<sup>2–9</sup> Self-initiation of acrylates at high temperatures improves the polymer quality and reduces the operating costs due to less or no use of expensive conventional initiators.<sup>10–17</sup>

Molecular oxygen is known to affect free-radical polymerization strongly.<sup>18</sup> Studying and conducting polymerization without considering the importance and involvement of oxygen leads to an incomplete understanding of the polymerization pathways. A practical concern about the participation of gaseous oxygen in polymerization is its ability to inhibit initiation.<sup>19</sup> Atmospheric oxygen can quench excited triplet-state initiators that provide free radicals during the initiation step, resulting in induction periods.<sup>20–22</sup> The reaction of oxygen molecules with carbon-based secondary propagating radicals generates peroxy ( $R-O-O^{\bullet}$ ) radicals, which are much less reactive and have

lower polymerization rates. Oxygen may also create peroxides or polyperoxides as copolymers with vinyl-type monomers,<sup>23</sup> which are unfavorable for polymerization reactions as well. Different approaches have been developed to mitigate the problem of oxygen inhibition. Physical approaches, such as bubbling and blanketing the reaction medium with inert gas (e.g., nitrogen),<sup>20,24</sup> or introducing barriers against atmospheric oxygen with waxes<sup>25</sup> or polymers (e.g., polyethylene)<sup>19</sup> with low oxygen permeability, are difficult and expensive methods to implement on an industrial scale.

Oxygen has also been reported to act as an initiator. For high-pressure polymerization of ethylene, induction time was observed to decrease with increasing oxygen concentration and temperature.<sup>26–28</sup> Grimsby and Gilliland<sup>29</sup> and Schoenemann<sup>30</sup> proposed that an oxygen molecule reacts with an ethylene molecule to produce two free radicals for propagation. Moreover, oxygen in combination with various organometallic chemicals (especially group III) generates high-performance initiators for free-radical polymerization.<sup>18</sup> For instance, trialkylborane alone cannot polymerize the vinyl-based mono-

**Received:** April 1, 2021

**Revised:** July 11, 2021

**Published:** August 16, 2021



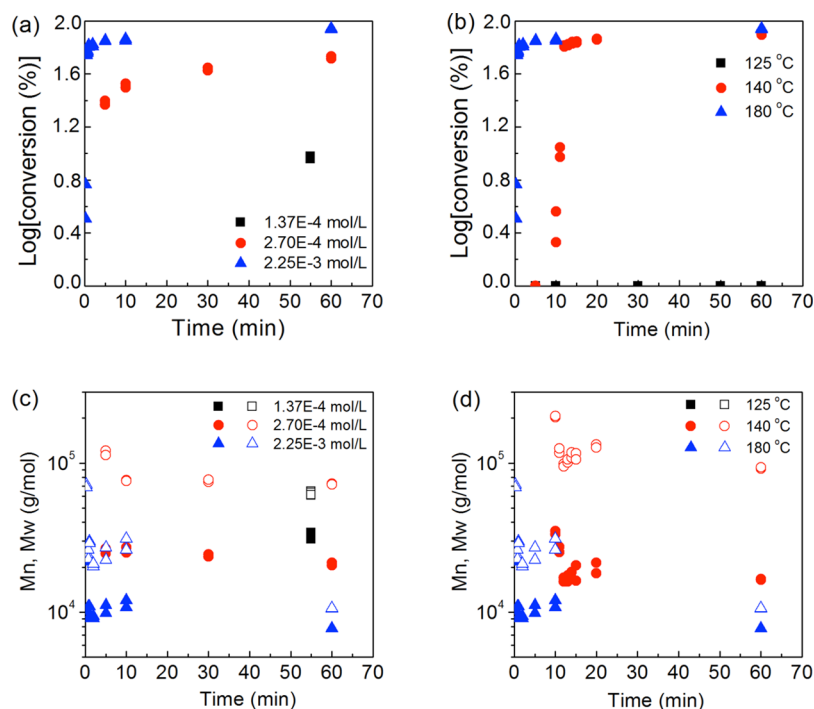


**Figure 1.** (a) Log of *n*BA conversion vs time at 180 °C: black squares, red circles, and blue triangles for the monomer with  $1.37 \times 10^{-4}$ ,  $2.70 \times 10^{-4}$ , and  $2.25 \times 10^{-3}$  mol/L dissolved O<sub>2</sub>, respectively. (b) Log of conversion of air-saturated *n*BA vs time at different temperatures. No conversion is observed at 125 °C. (c) Number-average (filled symbols) and weight-average (empty symbols) molecular weights of the polymer samples in (a). (d) Number-average (filled symbols) and weight-average molecular (empty symbols) weights of the polymer samples in (b).

mers, yet polymerization occurs when oxygen is added.<sup>14</sup> Recent work has also demonstrated diatomic oxygen's role in initiation by activating trialkylborane even in the absence of organometallic species and at ambient conditions.<sup>31,32</sup> Oxygen also plays a pivotal role in methyl methacrylate polymerization initiated by a copper(II)-ascorbic acid-oxygen system in aqueous medium.<sup>33,34</sup>

In this study for the first time, we report free-radical polymerization of *n*-butyl acrylate (*n*BA) at different O<sub>2</sub> concentrations and at high temperatures (140–180 °C) in the absence of any added thermal- or photo-initiators. Monomer conversion measurements indicate that *n*BA saturated with air polymerizes vigorously and that the rate of polymerization increases with increasing oxygen concentration and temperature. Using quantum chemical calculations based on density functional theory (DFT), we understand how oxygen reacts with alkyl acrylate monomers to produce and sustain radicals for initiation. DFT calculations show that at high temperatures, peroxy radicals decompose with molecular oxygen dissociating from the monomer complex to recover active carbon-based secondary radicals. These results suggest that oxygen acts as an initiator and catalyst for alkyl acrylate free-radical polymerization at  $T > 140$  °C.

## RESULTS AND DISCUSSION

We explore the temperature dependence of the spontaneous bulk thermal polymerization of *n*BA with three different dissolved oxygen concentrations. The procedure for removal of inhibitors and all experimental methods, including measuring the oxygen content, have been explained in S1 of Supporting Information. From our previous study, we understood that at 140 °C, there is less than 3% conversion of ultra-high purity (UHP) N<sub>2</sub>-bubbled *n*BA monomer after 240 min.<sup>35</sup> However,

the polymerization rate increased with increasing temperature. At 220 °C, polymerization continues beyond 250 min. The monomer self-initiation rate coefficient increases from  $2.2 \times 10^{-14} \text{ M}^{-1} \text{ s}^{-1}$  at 160 °C to  $6.8 \times 10^{-12} \text{ M}^{-1} \text{ s}^{-1}$  at 220 °C. These findings, obtained at negligible concentrations of oxygen without solvent, suggested that the monomer self-initiation reaction is intrinsically slow and only plays an appreciable role at  $T > 160$  °C.

Free-radical bulk polymerization of *n*BA bubbled with UHP N<sub>2</sub> for various purging times (to adjust oxygen concentration) is conducted at high temperatures to investigate the participation of O<sub>2</sub> and differentiate this study from conventional studies on acrylate free-radical bulk polymerization.<sup>17,35–38</sup> Figure 1a shows that while 10% of the deaerated *n*BA ( $1.37 \times 10^{-4}$  mol/L oxygen) is converted to polymer after 60 min at 180 °C, a conversion of 50% can be achieved in only 30 s for the air-saturated *n*BA ( $2.25 \times 10^{-3}$  mol/L oxygen). This suggests that oxygen accelerates polymerization significantly and that higher O<sub>2</sub> concentrations also increase the monomer conversion. After 1 hour, the final conversion of air-saturated monomer is 86%, which is more than 8.5 times higher than that for deaerated *n*BA at the same temperature. This suggests that molecular oxygen increases the polymerization rate substantially at 180 °C, which highlights the importance of oxygen in free-radical polymerization at high temperatures.

In order to investigate the temperature dependence, *n*BA saturated with oxygen was polymerized at different temperatures as shown in Figure 1b. At 125 °C, oxygen appears to act as an inhibitor. This temperature is simply too low for initiation with O<sub>2</sub>. It is obvious that the spontaneous polymerization rate increases rapidly with temperature and that monomer conversion grows from 78% at 140 °C to 86% at 180 °C. Note that the conversion increases very sharply initially. After

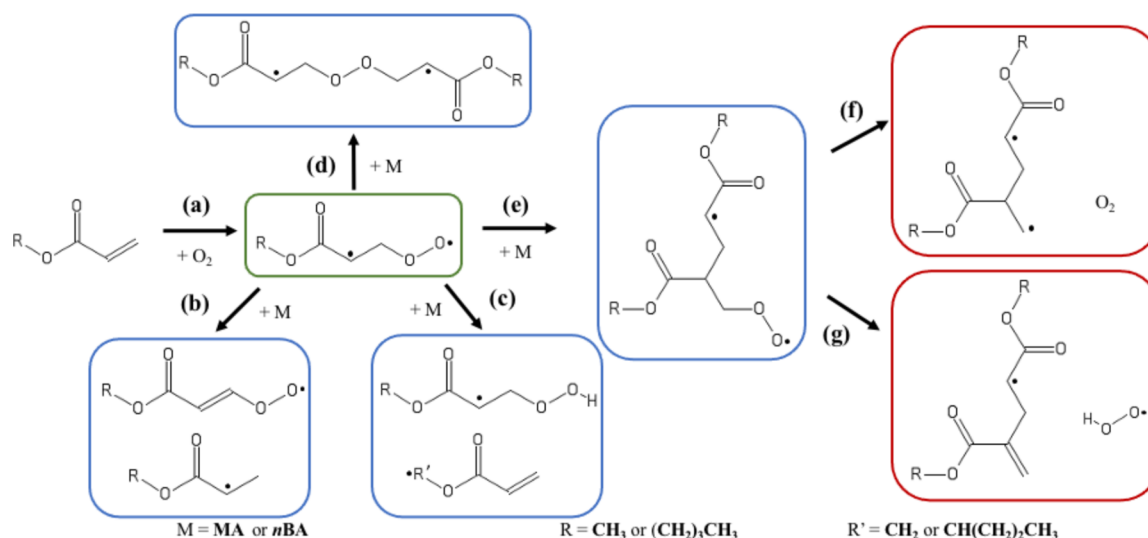


**Figure 2.** (a) Oxygen addition to the monomer forming a diradical intermediate, (b) radical transfer from a secondary carbon to the monomer, (c) radical transfer from peroxy to the monomer, (d) diradical propagation via the peroxy radical, (e) diradical propagation via the secondary-carbon radical, (f) C–O<sub>2</sub> bond dissociation, and (g) mono-radical generation by release of •OOH. Corresponding activation energies and rate constants are given in Table 2.

this sharp increase, it increases at a much slower rate and reaches only 86% after 1 h because the viscosity of the reaction media increases sharply with increased conversion, making the reaction diffusion limited (preventing the monomer molecules from reaching free radicals readily). We carried out the same polymerization in the presence of *n*-heptane that does not participate in the polymerization, and we were able to achieve 100% conversion.

An induction period where time passes before considerable conversion is observed for 140–180 °C. The induction time significantly declines as temperature rises from 11 min for 140 °C to less than 15 s for 180 °C. After the induction time, a nearly vertical increase in conversion implies that free-radical polymerization of air-saturated *n*BA is remarkably fast. Figure 1c,d shows the number-average and weight-average molecular weights of the polymer samples, the conversions of which are depicted in Figure 1a,b, respectively. These figures confirm that the polymerization reactions produced long-chain polymers.

To understand the role of oxygen in high-temperature polymerization of alkyl acrylates, we also carry out a systematic, first-principles exploration with GAMESS<sup>39</sup> using DFT, the Becke-3-Lee-Young-Parr hybrid functional (B3LYP), and the 6-311G\*\* basis set. Further details on computational methods are given in S2 of Supporting Information. Previous studies employ B3LYP, and its use is well validated for alkyl acrylate and free-radical investigations.<sup>6,7,11,13,40</sup> The solvation entropy is calculated for aerated experimental conditions ([O<sub>2</sub>] = 2.1 × 10<sup>-3</sup> mol/L) and is accounted for in reaction entropies involving molecular oxygen (see S2.4 of Supporting Information). Given the chemical similarity of methyl acrylate (MA) and *n*BA, we first study various possible reactions of an MA molecule and a triplet ground-state O<sub>2</sub> (see Figure S2). Molecular oxygen may react with the vinyl group of MA by Markovnikov addition, producing a reactive, carbon-based secondary radical and a terminal peroxy radical (see Figure 2). O<sub>2</sub> is favored to form a bond with the β-carbon of MA due to the greater stability of the resulting secondary radical.

Because oxygen inhibits free-radical polymerization at low temperatures, peroxy formation (•M–H + •OO• → •OOMH)

and peroxy dissociation (•OOMH → •M–H + •OO•) were first studied where M = MA. Thermodynamic parameters and rate constants were calculated using the methods highlighted in S2.3 and S2.5 of Supporting Information, respectively. •M–H type mono-radicals result from self-initiation mechanisms<sup>40</sup> and therefore are chosen for this study. DFT calculations predict an electronic energy barrier of 94.21 kJ/mol for peroxy formation.

With increased temperature, the rate constant of peroxy formation decreases appreciably, while the rate constant of the reverse reaction increases (Table 1). At 25 °C, the rate constant

**Table 1.** Enthalpy (Δ*H*) and Gibbs Free Energy (Δ*G*) in kJ/mol, Entropy (Δ*S*) in J/mol K, and Rate Constants *k*(*T*) at Various Temperatures for Peroxy Formation (Forward) and Dissociation (Reverse) Reactions for O<sub>2</sub> and MA Mono-Radical (•M–H)<sup>a</sup>

<i>T</i> (°C)	Δ <i>H</i> <sub>forward</sub>	Δ <i>S</i> <sub>forward</sub>	Δ <i>G</i> <sub>forward</sub>	<i>k</i> <sub>forward</sub> ( <i>T</i> ) (M <sup>-1</sup> s <sup>-1</sup> )	<i>k</i> <sub>reverse</sub> ( <i>T</i> ) (s <sup>-1</sup> )
25	-102.8	-121.2	-66.7	7.5 × 10 <sup>27</sup>	1.3 × 10 <sup>1</sup>
100	-105.0	-121.4	-59.7	5.5 × 10 <sup>24</sup>	3.4 × 10 <sup>4</sup>
120	-105.6	-121.4	-57.9	1.3 × 10 <sup>24</sup>	1.7 × 10 <sup>5</sup>
140	-106.2	-121.3	-56.1	3.7 × 10 <sup>23</sup>	7.0 × 10 <sup>5</sup>
180	-107.3	-121.1	-52.5	4.0 × 10 <sup>22</sup>	8.4 × 10 <sup>6</sup>
200	-107.9	-120.9	-50.7	1.6 × 10 <sup>22</sup>	2.5 × 10 <sup>7</sup>

<sup>a</sup>Note: for brevity, Δ*H*<sub>reverse</sub>, Δ*S*<sub>reverse</sub>, and Δ*G*<sub>reverse</sub> omitted as Δ*H*<sub>reverse</sub> = -Δ*H*<sub>forward</sub> and so forth.

of peroxy formation is approximately 26 orders of magnitude faster than the corresponding dissociation reaction. However, at 200 °C, the rate constant for peroxy formation is favored over dissociation by 15 orders of magnitude instead. The faster rate constant of peroxy dissociation at high temperatures may be attributed to the positive entropic consequence of splitting one molecule into two. The kinetic boost that peroxy dissociation gains with increased thermal energy frees dissolved oxygen to interact more readily with the unreacted monomer. These results suggest that molecular oxygen's role as an inhibitor—forming peroxy species—decreases at elevated temperatures. This computational insight can help explain the induction

**Table 2. Activation Energy ( $E_A$ ) and Gibbs Free Energy ( $\Delta G^\ddagger$ ) in kJ/mol, Entropy ( $\Delta S^\ddagger$ ) in J/mol K, and Rate Constants  $k(T)$  at 140 °C for Oxygen-Monomer Reactions, as Shown in Figure 2, for MA (Shading) and *n*BA (No Shading)**

	Initiation	Mono-Radical Generation		Diradical Propagation		Peroxyl Radical Dissociation	
	(a)	(b)	(c)	(d)	(e)	(f) <sup>a</sup>	(g)
$E_A$	121.6	85.6	75.1	31.5	16.7	146.8	118.5
	121.1	85.4	63.4	31.4	15.6	146.7	118.9
$\Delta G^\ddagger$	155.4	146.5	133.4	97.6	76.1	102.4	119.7
	161.8	157.6	127.4	108.8	84.6	106.1	121.4
$\Delta S^\ddagger$	-98.3	-164.0	-157.8	-176.5	-160.6	136.4	-11.5
	-115.3	-191.5	-171.7	-203.9	-183.6	127.1	-14.3
$k(T)$	$7.6 \times 10^{-9}$	$2.8 \times 10^{-7}$	$9.4 \times 10^{-6}$	$1.6 \times 10^{-1}$	$7.5 \times 10^1$	$3.3 \times 10^3$	$9.5 \times 10^{-3}$
	$M^{-1}s^{-1}$	$M^{-1}s^{-1}$	$M^{-1}s^{-1}$	$M^{-1}s^{-1}$	$M^{-1}s^{-1}$	$s^{-1}$	$s^{-1}$
	$1.2 \times 10^{-9}$	$1.1 \times 10^{-8}$	$5.5 \times 10^{-5}$	$6.0 \times 10^{-3}$	6.4	$1.1 \times 10^3$	$5.9 \times 10^{-3}$
	$M^{-1}s^{-1}$	$M^{-1}s^{-1}$	$M^{-1}s^{-1}$	$M^{-1}s^{-1}$	$M^{-1}s^{-1}$	$s^{-1}$	$s^{-1}$

<sup>a</sup> $\Delta E_0$  in place of  $E_A$ ;  $\Delta G_{\text{rxn}}$  and  $\Delta S_{\text{rxn}}$  in place of  $\Delta G^\ddagger$  and  $\Delta S^\ddagger$ , respectively (see S2.5 of Supporting Information).

period observed in the experiment at 140 °C as both inhibitory and initiator behaviors are observed. Yet, at 180 °C, the lack of a measurable induction period may be attributed to the inhibitory role of oxygen decreasing as it is freed from quenching radicals more readily.

The possible reactions stemming from the active triplet-diradical intermediate formed after oxygen addition to the monomer are explored for both MA and *n*BA homo-polymerization (Figure 2). Table 2 reports the activation energies and rate constants, calculated with DFT using B3LYP/6-311G\*\* and transition-state theory, relevant to the initiation of MA and *n*BA polymerization at 140 °C. Detailed tables for 120, 140, 180, and 200 °C are given in S3 of Supporting Information. We find that the initiation step, oxygen addition to the C=C double bond of the acrylate, is kinetically and thermodynamically rate limiting. For both MA and *n*BA polymerization, this step has a high activation energy of 121.6 and 121.1 kJ/mol and a relatively low rate constant of  $7.4 \times 10^{-9}$  and  $1.2 \times 10^{-9} M^{-1} s^{-1}$ , respectively. A low rate constant is expected as adsorption of molecular oxygen onto a monomer is penalized for a significantly negative activation entropy.

However, as temperature increases, the oxygen addition rate constant counterintuitively increases to  $2.4 \times 10^{-7} M^{-1} s^{-1}$  at 180 °C for MA, demonstrating opposite trends to that of radical termination with  $O_2$ , as listed in Table 1. While both rate constants are reduced by the entropic cost of gas adsorption, the activation entropy of the Markovnikov addition is less negative than the reaction entropy of  $O_2$  radical termination. This trend suggests that elevated temperatures favor oxygen initiation while hindering oxygen inhibition, which agrees with experimental observations despite the relatively low theoretical rate constant. It is also noted that the oxygen-MA initiation reaction is still 5–6 orders of magnitude faster than self-initiation, which has a non-adiabatic rate constant of  $1.1 \times 10^{-14} M^{-1} s^{-1}$  at 140 °C due to a slow intersystem crossing process (singlet–triplet crossover) limited by the small spin–orbit coupling of hydrocarbons.<sup>40,41</sup> It, therefore, becomes more favorable for  $O_2$  to initiate MA and *n*BA polymerization rather than for monomers to self-initiate at elevated temperatures.

Following oxygen initiation, it is more likely that propagation reactions, having low activation energy barriers, next take place as opposed to mono-radical generation shown in Figure 2b,c. It is noted here that  $\bullet OH$  is not expected to be generated as the abstraction of a hydrogen by the peroxy radical has a slow rate constant for both MA and *n*BA (Table 2). Propagation of both radical sites may occur at high temperatures, where a moderate rate constant of  $1.6 \times 10^{-1} M^{-1} s^{-1}$  follows for the peroxy radical

and a relatively fast rate constant of  $7.5 \times 10^1 M^{-1} s^{-1}$  follows for the secondary carbon-based radical in MA polymerization. Diradical propagation reactions for *n*BA are observed to yield rate constants 2 orders of magnitude slower than MA. As expected, the peroxy radical is much less active (2 orders of magnitude slower) than the carbon radical toward chain propagation for both MA and *n*BA polymerization. This may translate into highly asymmetric chain growth, with the peroxy radical capping at one end.

Few peroxide species of the type  $\bullet MOOM\bullet$  are expected to be generated over the course of the reaction. Additionally, this triplet diradical is not favored for O–O dissociation, having a calculated bond dissociation energy (BDE) of 210 kJ/mol, which is high relative to the energy barriers of the pathways proposed here. The high BDE may be attributed to the triplet product  $\bullet MO\bullet$  being a high energy intermediate due to the proximity of its radical centers. This BDE is comparable to those of studied peroxides, both experimentally and by other DFT studies.<sup>42</sup> The rate constant of forming  $\bullet MO\bullet$  is  $1.4 \times 10^{-3} s^{-1}$  for  $M = MA$  at 140 °C, which is rather slow. Therefore,  $R-O\bullet$  type initiator species are not predicted to be generated by this mechanism, reducing the likelihood of  $O_2$  being consumed over the course of the reaction.

The oxygen atoms can then leave the live chain two ways, either by C– $O_2$  bond thermal dissociation or by releasing  $\bullet OOH$ . Here, the theoretical C– $O_2$  BDE is 147 kJ/mol, which is comparable to the R– $OO\bullet$  dissociation energy of similar alkyl peroxides [e.g., *n*-butyl peroxy radical  $CH_3(CH_2)_3-OO\bullet$ ,  $145 \pm 4$  kJ/mol].<sup>43</sup> Furthermore, despite the large activation energy, the rate constant for C– $O_2$  dissociation is relatively fast for both MA and *n*BA due to the significant, positive contribution of entropy to the reaction free energy. As shown in Figure 2g, the peroxy radical abstracts one hydrogen atom from its backbone and then dissociates. This reaction also has a moderately slow rate constant of  $9.5 \times 10^{-3}$  and  $5.9 \times 10^{-3} s^{-1}$  for MA and *n*BA, respectively, making it less likely to occur at high temperatures. The reaction's activation entropy is less favorable than the reaction entropy of C– $O_2$  thermal dissociation because of the backbiting mechanism's low entropy, coordinated transition state that forms an O–H bond while breaking a C–O bond. It is therefore suggested that  $O_2$  returns to the reaction medium as a true catalyst by C– $O_2$  thermal dissociation. Molecular oxygen is predicted to leave the two-monomer-unit diradical and return to the reaction media, thus acting as an initiator/catalyst. The diradical product can then react with a third monomer to generate two mono-radicals. This finding is supported by experimental observation that at high temperatures, a very low



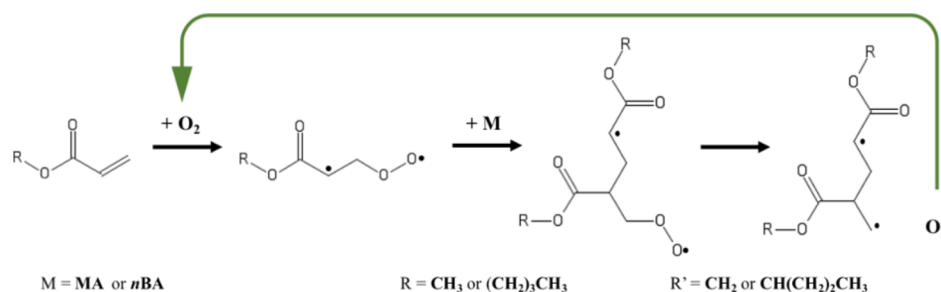


**Figure 3.** Catalytic role of molecular oxygen in MA and *n*BA polymerization.

concentration of  $\text{O}_2$  vigorously initiates and sustains polymerization. The overall catalytic pathway of  $\text{O}_2$  in MA and *n*BA polymerization is illustrated in Figure 3.

## CONCLUSIONS

Using DFT calculations, the known inhibiting role of  $\text{O}_2$  in free-radical polymerization was found to diminish substantially with increased temperature. These theoretical findings are in agreement with our experimental observations at  $T > 140$  °C that show the presence of molecular oxygen dramatically increases the polymerization rate in comparison to the monomer self-initiation processes. Particularly, we showed that the conversion of the deaerated monomer is significantly less than that of the air-saturated monomer at 180 °C. Our DFT studies provide insights into the mechanism of MA and *n*BA free-radical polymerization in the presence of molecular oxygen. First,  $\text{O}_2$  initiates polymerization by bonding to the monomer vinyl group to form an active triplet diradical. Another monomer is then attached via propagation off the reactive secondary-carbon radical. Finally,  $\text{O}_2$  leaves by thermal dissociation. This sequence of reactions illustrates the catalytic role of  $\text{O}_2$ . The first step, oxygen addition to the monomer, was predicted to be the rate-limiting step due to the entropic cost of dissolved gas adsorption; however, this step becomes faster at elevated temperatures, in agreement with experimental observations. Molecular oxygen is then favored to leave dimerized monomers by C– $\text{O}_2$  bond dissociation because of the high entropic gain. The oxygen-initiation mechanism provides a faster reaction pathway for mono-radical generation compared to thermal self-initiation. Thus, oxygen-catalyzed initiation of free-radical polymerization of alkyl acrylates is promising for future cost-efficient and sustainable polymer production.

## ASSOCIATED CONTENT

### Supporting Information

The Supporting Information is available free of charge at <https://pubs.acs.org/doi/10.1021/acs.macromol.1c00669>.

Further descriptions of experimental and computational methods, select energies of optimized structures, and additional information on kinetic parameters (PDF)

All optimized structures (ZIP)

## AUTHOR INFORMATION

### Corresponding Authors

Masoud Soroush – Department of Chemical and Biological Engineering, Drexel University, Philadelphia, Pennsylvania 19104-2816, United States; Email: [soroushm@drexel.edu](mailto:soroushm@drexel.edu)

Andrew M. Rappe – Department of Chemistry, University of Pennsylvania, Philadelphia, Pennsylvania 19104-6323,

United States; [orcid.org/0000-0003-4620-6496](https://orcid.org/0000-0003-4620-6496);  
Email: [rappe@sas.upenn.edu](mailto:rappe@sas.upenn.edu)

## Authors

Shi Liu – School of Science, Westlake University, Hangzhou, Zhejiang 310024, China; Institute of Natural Sciences, Westlake Institute for Advanced Study, Hangzhou, Zhejiang 310024, China; Department of Chemistry, University of Pennsylvania, Philadelphia, Pennsylvania 19104-6323, United States; [orcid.org/0000-0002-8488-4848](https://orcid.org/0000-0002-8488-4848)

Lauren Chua – Department of Chemistry, University of Pennsylvania, Philadelphia, Pennsylvania 19104-6323, United States; [orcid.org/0000-0001-8065-2989](https://orcid.org/0000-0001-8065-2989)

Ahmad Arabi Shamsabadi – Department of Chemical and Biological Engineering, Drexel University, Philadelphia, Pennsylvania 19104-2816, United States

Patrick Corcoran – Department of Chemical and Biological Engineering, Drexel University, Philadelphia, Pennsylvania 19104-2816, United States

Abhirup Patra – Department of Chemistry, University of Pennsylvania, Philadelphia, Pennsylvania 19104-6323, United States; [orcid.org/0000-0002-2446-8017](https://orcid.org/0000-0002-2446-8017)

Michael C. Grady – Axalta Coating Systems, Global Innovation Center, Philadelphia, Pennsylvania 19112, United States

Complete contact information is available at:

<https://pubs.acs.org/doi/10.1021/acs.macromol.1c00669>

## Author Contributions

#S.L. and L.C. contributed equally to this work.

## Notes

The authors declare no competing financial interest.

## ACKNOWLEDGMENTS

This material is based upon work supported by the U.S. National Science Foundation under grant nos. CBET-1803215 and CBET-1804285. Any opinions, findings, and conclusion or recommendations expressed in this material are those of the authors and do not necessarily reflect the views of the National Science Foundation. The theoretical work of S.L., L.C., A.P., and A.M.R. was supported by the grant CBET-1803215, and the experimental work of A.A.S., P.C., M. G., and M.S. was supported by the grant CBET-1804285.

## REFERENCES

- (1) Conner, L. Economic impact and regulatory flexibility analyses of the final architectural coatings VOC rule, 1998. <https://www.osti.gov/biblio/305776>.
- (2) Grady, M. C.; Simonsick, W. J.; Hutchinson, R. A. Studies of higher temperature polymerization of *n*-butyl methacrylate and *n*-butyl acrylate. *Macromol. Symp.* **2002**, *182*, 149–168.

- (3) Wang, W.; Hutchinson, R. A. Recent Advances in the Study of High-Temperature Free Radical Acrylic Solution Copolymerization. *Macromol. React. Eng.* **2008**, *2*, 199–214.
- (4) Riazi, H.; Arabi Shamsabadi, A.; Grady, M. C.; Rappe, A. M.; Soroush, M. Method of Moments Applied to Most-Likely High-Temperature Free-Radical Polymerization Reactions. *Processes* **2019**, *7*, 656.
- (5) Junkers, T.; Barner-Kowollik, C. The role of mid-chain radicals in acrylate free radical polymerization: Branching and scission. *J. Polym. Sci., Part A: Polym. Chem.* **2008**, *46*, 7585–7605.
- (6) Cuccato, D.; Mavrouidakis, E.; Dossi, M.; Moscatelli, D. A Density Functional Theory Study of Secondary Reactions in n-Butyl Acrylate Free Radical Polymerization. *Macromol. Theory Simul.* **2013**, *22*, 127–135.
- (7) Liu, S.; Srinivasan, S.; Grady, M. C.; Soroush, M.; Rappe, A. M. Backbiting and  $\beta$ -scission reactions in free-radical polymerization of methyl acrylate. *Int. J. Quantum Chem.* **2014**, *114*, 345–360.
- (8) Riazi, H.; Shamsabadi, A.; Rappe, A. M.; Soroush, M. Experimental and Theoretical Study of the Self-Initiation Reaction of Methyl Acrylate in Free-Radical Polymerization. *Ind. Eng. Chem. Res.* **2018**, *57*, 532–539.
- (9) Ballard, N.; Asua, J. M. Radical polymerization of acrylic monomers: An overview. *Prog. Polym. Sci.* **2018**, *79*, 40–60.
- (10) Quan, C.; Soroush, M.; Grady, M. C.; Hansen, J. E.; Simonsick, W. J. High-Temperature Homopolymerization of Ethyl Acrylate and n-Butyl Acrylate: Polymer Characterization. *Macromolecules* **2005**, *38*, 7619–7628.
- (11) Srinivasan, S.; Lee, M. W.; Grady, M. C.; Soroush, M.; Rappe, A. M. Self-initiation mechanism in spontaneous thermal polymerization of ethyl and n-butyl acrylate: a theoretical study. *J. Phys. Chem. A* **2010**, *114*, 7975–7983.
- (12) Srinivasan, S.; Kalfas, G.; Petkovska, V. I.; Bruni, C.; Grady, M. C.; Soroush, M. Experimental study of the spontaneous thermal homopolymerization of methyl and n-butyl acrylate. *J. Appl. Polym. Sci.* **2010**, *118*, 1898–1909.
- (13) Srinivasan, S.; Lee, M. W.; Grady, M. C.; Soroush, M.; Rappe, A. M. Computational evidence for self-initiation in spontaneous high-temperature polymerization of methyl methacrylate. *J. Phys. Chem. A* **2011**, *115*, 1125–1132.
- (14) Zorn, A.-M.; Junkers, T.; Barner-Kowollik, C. Synthesis of a Macromonomer Library from High-Temperature Acrylate Polymerization. *Macromol. Rapid Commun.* **2009**, *30*, 2028–2035.
- (15) Junkers, T.; Bennet, F.; Koo, S. P. S.; Barner-Kowollik, C. Self-directed formation of uniform unsaturated macromolecules from acrylate monomers at high temperatures. *J. Polym. Sci., Part A: Polym. Chem.* **2008**, *46*, 3433–3437.
- (16) Laki, S.; Shamsabadi, A.; Grady, M. C.; Rappe, A. M.; Soroush, M. Experimental and Mechanistic Modeling Study of Self-Initiated High-Temperature Polymerization of Ethyl Acrylate. *Ind. Eng. Chem. Res.* **2020**, *59*, 2621–2630.
- (17) Riazi, H.; Shamsabadi, A. A.; Corcoran, P.; Grady, M. C.; Rappe, A. M.; Soroush, M. On the Thermal Self-Initiation Reaction of n-Butyl Acrylate in Free-Radical Polymerization. *Processes* **2018**, *6*, 3.
- (18) Bhanu, V. A.; Kishore, K. Role of Oxygen in Polymerization Reactions. *Chem. Rev.* **1991**, *91*, 99–117.
- (19) Ligon, S. C.; Husár, B.; Wutzel, H.; Holman, R.; Liska, R. Strategies to Reduce Oxygen Inhibition in Photoinduced Polymerization. *Chem. Rev.* **2014**, *114*, 557–589.
- (20) Wight, F. R. Oxygen inhibition of acrylic photopolymerization. *J. Polym. Sci., Polym. Lett. Ed.* **1978**, *16*, 121–127.
- (21) Chong, J. S. Oxygen consumption during induction period of a photopolymerizing system. *J. Appl. Polym. Sci.* **1969**, *13*, 241–247.
- (22) Decker, C.; Jenkins, A. D. Kinetic Approach of O<sub>2</sub> Inhibition in Ultraviolet- and Laser-Induced Polymerizations. *Macromolecules* **1985**, *18*, 1241–1244.
- (23) Bovey, F. A.; Kolthoff, I. M. The Mechanism of Emulsion Polymerizations. III. Oxygen as a Comonomer in the Emulsion Polymerization of Styrene. *J. Am. Chem. Soc.* **1947**, *69*, 2143–2153.
- (24) Krongauz, V. V.; Chawla, C. P.; Dupre, J. *Photoinitiated Polymerization*; 2003; Chapter 14, pp 165–175.
- (25) Bolon, D. A.; Webb, K. K. Barrier coats versus inert atmospheres. The elimination of oxygen inhibition in free-radical polymerizations. *J. Appl. Polym. Sci.* **1978**, *22*, 2543–2551.
- (26) Fawcett, E. W.; Gibson, R.; Perrin, M.; Paton, J.; Williams, E. *Chem. Abstr.* **1938**, *32*, 13626.
- (27) Ehrlich, P.; Pittilo, R. N. A kinetic study of the oxygen-initiated polymerization of ethylene. *J. Polym. Sci.* **1960**, *43*, 389–412.
- (28) Tatsukami, Y.; Takahashi, T.; Yoshioka, H. Reaction mechanism of oxygen-initiated ethylene polymerization at high pressure. *Die Makromolekulare Chem.* **1980**, *181*, 1107–1114.
- (29) Grimsby, F. N.; Gilliland, E. Continuous Oxygen-Initiated Ethylene Polymerization. *Ind. Eng. Chem.* **1958**, *50*, 1049–1052.
- (30) Schoenemann, K. Bewährte arbeitsprinzipien für die Berechnung chemischer Reaktoren. *Chem. Eng. Sci.* **1963**, *18*, 565–581.
- (31) Kim, C. S.; Cho, S.; Lee, J. H.; Cho, W. K.; Son, K.-s. Open-to-Air RAFT Polymerization on a Surface under Ambient Conditions. *Langmuir* **2020**, *36*, 11538–11545.
- (32) Lv, C.-N.; Li, N.; Du, Y.-X.; Li, J.-H.; Pan, X.-C. Activation and Deactivation of Chain-transfer Agent in Controlled Radical Polymerization by Oxygen Initiation and Regulation. *Chin. J. Polym. Sci.* **2020**, *38*, 1178–1184.
- (33) Reddy, G. G.; Nagabhushanam, T.; Venkata Rao, K.; Santappa, M. Polymerization of methyl methacrylate in the presence of molecular oxygen — a kinetic study. *Polym* **1981**, *22*, 1692–1698.
- (34) Reddy, G. G.; Nagabhushanam, T.; Rao, K. V.; Santappa, M. Oxygen-ascorbic acid-ferric ion initiating system. Kinetics of polymerization of methyl methacrylate. *Die Angewandte Makromolekulare Chemie* **1983**, *115*, 61–74.
- (35) Shamsabadi, A. A.; Moghadam, N.; Srinivasan, S.; Corcoran, P.; Grady, M. C.; Rappe, A. M.; Soroush, M. Study of n-Butyl Acrylate Self-Initiation Reaction Experimentally and via Macroscopic Mechanistic Modeling. *Processes* **2016**, *4*, 15.
- (36) Nikitin, A. N.; Hutchinson, R. A. Effect of Intramolecular Transfer to Polymer on Stationary Free Radical Polymerization of Alkyl Acrylates. *2. Macromol. Theory Simul.* **2006**, *15*, 128–136.
- (37) Nikitin, A. N.; Hutchinson, R. A.; Wang, W.; Kalfas, G. A.; Richards, J. R.; Bruni, C. Effect of Intramolecular Transfer to Polymer on Stationary Free-Radical Polymerization of Alkyl Acrylates, 5 – Consideration of Solution Polymerization up to High Temperatures. *Macromol. React. Eng.* **2010**, *4*, 691–706.
- (38) Barth, J.; Buback, M.; Hesse, P.; Sergeeva, T. Termination and Transfer Kinetics of Butyl Acrylate Radical Polymerization Studied via SP-PLP-EPR. *Macromolecules* **2010**, *43*, 4023–4031.
- (39) Schmidt, M. W.; Baldrige, K. K.; Boatz, J. A.; Elbert, S. T.; Gordon, M. S.; Jensen, J. H.; Koseki, S.; Matsunaga, N.; Nguyen, K. A.; Su, S.; Windus, T. L.; Dupuis, M.; Montgomery, J. A. General Atomic and Molecular Electronic Structure System. *J. Comput. Chem.* **1993**, *14*, 1347–1363.
- (40) Srinivasan, S.; Lee, M. W.; Grady, M. C.; Soroush, M.; Rappe, A. M. Computational Study of the Self-Initiation Mechanism in Thermal Polymerization of Methyl Acrylate. *J. Phys. Chem. A* **2009**, *113*, 10787–10794.
- (41) Liu, S.; Srinivasan, S.; Tao, J.; Grady, M. C.; Soroush, M.; Rappe, A. M. Modeling Spin-Forbidden Monomer Self-Initiation Reactions in Spontaneous Free-Radical Polymerization of Acrylates and Methacrylates. *J. Phys. Chem. A* **2014**, *118*, 9310–9318.
- (42) Bach, R. D.; Schlegel, H. B. Bond Dissociation Energy of Peroxides Revisited. *J. Phys. Chem. A* **2020**, *124*, 4742–4751.
- (43) Simmie, J. M.; Black, G.; Curran, H. J.; Hinde, J. P. Enthalpies of Formation and Bond Dissociation Energies of Lower Alkyl Hydroperoxides and Related Hydroperoxy and Alkoxy Radicals. *J. Phys. Chem. A* **2008**, *112*, 5010–5016.